Dynamics of the BCS-BEC Crossover in a Degenerate Fermi Gas

M. H. Szymańska,[1] B. D. Simons,[1] and K. Burnett[2]

[1]*Cavendish Laboratory, University of Cambridge, Madingley Road, Cambridge CB3 OHE, United Kingdom*
[2]*Clarendon Laboratory, University of Oxford, Parks Road, Oxford, OX1 3PU, United Kingdom*

We study the short-time dynamics of a degenerate Fermi gas positioned near a Feshbach resonance following an abrupt jump in the atomic interaction resulting from a change of magnetic field. We investigate the dynamics of the condensate order parameter and pair wave function for a range of field strengths. When the jump is sufficient to span the BCS to Bose-Einstein condensation crossover, we show that the rigidity of the momentum distribution precludes any atom-molecule oscillations in the entrance channel dominated resonances observed in ^{40}K and ^{6}Li. Focusing on material parameters tailored to the ^{40}K Feshbach resonance at 202.1 G, we comment on the integrity of the fast sweep projection technique as a vehicle to explore the condensed phase in the crossover region.

Ultracold alkali atomic gases provide a valuable arena in which to explore molecular Bose-Einstein condensation (BEC) [1] and fermionic pair condensation [2,3]. Further, the facility to control interparticle interactions via a magnetically tuned Feshbach resonance (FR) provides a unique opportunity to investigate the BCS-BEC crossover and the dynamics of condensate formation. As well as the adiabatic association of molecules [1], both fast sweep "projections" of fermionic pair condensates onto the molecular BEC [2,3] and atom-molecule Ramsey fringes [4] have been reported in the recent literature. Lately, motivated by earlier work on the BCS system [5,6], it was shown [7,8] that the mean-field equations of motion of a Bose-Fermi (BF) model, commonly used to describe the FR system, are characterized by an integrable nonlinear dynamics. From these works, three striking predictions emerged: First, after an abrupt change in the strength of the pair interaction, the condensate order parameter exhibits substantial oscillations which range in magnitude between some initial state value, Δ_{I}, and that expected for the equilibrium final state Δ_{eq}. Second, in the absence of energy relaxation processes, these oscillations remain undamped, suggesting the potential to observe coherent atom-molecule oscillations in the FR system. Third, a spectral "hole-burning" phenomenon in the atomic momentum distribution, at one-half of the molecular binding energy, provides a signature of such oscillations [8].

In the following, we argue that this behavior rests on an auxiliary constraint that, in the present system, seems hard to justify. Drawing on the results of numerical analysis of the unconstrained dynamics, we show that, in the absence of relaxational processes, the oscillations of the order parameter are damped substantially, even at the level of mean field. When the abrupt change of the interaction spans the BCS-BEC crossover, for both the single-channel and BF systems, the magnitude of oscillations are small and die out, leaving Δ close to the initial, and much smaller than the equilibrium value, Δ_{eq}. The distribution remains essentially "frozen" and the hole-burning oscillations pre-

dicted in Ref. [8] do not occur. This rigidity of the initial state prevents BCS-BEC atom-molecule oscillations but validates fast sweep techniques [2] as a probe of the crossover region.

A full microscopic theory of FR phenomena relies on all matrix elements connecting different spin states. In practice, an accurate description of the resonance can be obtained by using a magnetic field dependent effective interaction between atoms in the entrance channel or, more generally, in the two most relevant channels. For low relative momenta, relevant to cold atom physics, the full form of complex atomic potentials are not resolved. Indeed, separable potentials with parameters drawn from experiment and exact multichannel calculations can be used to recover all low-energy binary scattering observables [9,10]. As often only one bound state of the closed channel potential is relevant, it has been traditionally replaced by a fictitious Bose particle and FR phenomena captured by a BF Hamiltonian [11].

For the entrance channel dominated resonances observed in ^{40}K and ^{6}Li formal calculations [9,10] support a picture in which the BCS-BEC crossover is mediated by only a small admixture of closed channel states—in the ^{40}K FR at 202.1 G, the admixture of the closed channel is less than 8% of the total [10]. In fact, the weakly bound molecular state appears at a detuning E_0 which lies far from the value where the resonance state of the closed channel crosses the dissociation threshold. Since the two-body observables drawn from the exact numerical solution of the Shrödinger equation within finite-range single- and two-channel models do not differ over a wide range of fields [10], FR phenomena in ^{40}K can be equally well described by a single-channel theory,

$$\hat{H} = \sum_{\mathbf{k}s} \epsilon_{\mathbf{k}} a^{\dagger}_{\mathbf{k}s} a_{\mathbf{k}s} + \sum_{\mathbf{k}\mathbf{k}'\mathbf{q}} V_{\mathbf{k}\mathbf{k}'} a^{\dagger}_{\mathbf{k}+\mathbf{q}\uparrow} a^{\dagger}_{-\mathbf{k}\downarrow} a_{-\mathbf{k}'\downarrow} a_{\mathbf{k}'+\mathbf{q}\uparrow}, \quad (1)$$

involving Fermi operators $a^{\dagger}_{\mathbf{k}s}$ and $a_{\mathbf{k}s}$. In the following, to account for the entire region of the crossover (and not only

the universal regime), we take as matrix elements $V_{\mathbf{kk}'} = V_0(B)\chi_{\mathbf{k}}(\sigma_{\mathrm{bg}})\chi_{\mathbf{k}'}(\sigma_{\mathrm{bg}})$ with $\chi_{\mathbf{k}}(\sigma_{\mathrm{bg}}) = \exp[-(\mathbf{k}\sigma_{\mathrm{bg}})^2/2]$ and the parameters $V_0(B)$ and σ_{bg} chosen to recover the correct magnetic field dependence of the scattering length and the energy of the highest vibrational bound state [10].

The Heisenberg equations of motion are

$$i\dot{\kappa}_{\mathbf{k}} = 2\epsilon_{\mathbf{k}}\kappa_{\mathbf{k}} - \Delta_{\mathbf{k}}(2\Phi_{\mathbf{k}} - 1),$$
$$i\dot{\Phi}_{\mathbf{k}} = \Delta_{\mathbf{k}}\kappa_{\mathbf{k}}^{\star} - \Delta_{\mathbf{k}}^{\star}\kappa_{\mathbf{k}},\tag{2}$$

where $\Phi_{\mathbf{k}} = \frac{1}{2}\sum_s\langle a_{\mathbf{ks}}^{\dagger}a_{\mathbf{ks}}\rangle$, $\kappa_{\mathbf{k}} = \langle a_{-\mathbf{k}\downarrow}a_{\mathbf{k},\uparrow}\rangle$, and $\Delta_{\mathbf{k}} = V_0(B)\chi_{\mathbf{k}}(\sigma_{\mathrm{bg}})\sum_{\mathbf{k}'}\chi_{\mathbf{k}'}(\sigma_{\mathrm{bg}})\kappa_{\mathbf{k}'}$ denotes the complex order parameter. Similarly for a BF theory, defining $g_{\mathbf{k}} = g_0\chi_{\mathbf{k}}(\sigma)$ as the coupling of the entrance channel to the bosonic field $b_{\mathbf{k}}$ associated with the Feshbach resonance level of the closed channel, the equations acquire the same form as (2) with $\Delta_{\mathbf{k}} = g_0\chi_{\mathbf{k}}(\sigma)b_0 + V_{\mathrm{bg}}\chi_{\mathbf{k}}(\sigma_{\mathrm{bg}})\sum_{\mathbf{k}'}\chi_{\mathbf{k}'}(\sigma_{\mathrm{bg}})\kappa_{\mathbf{k}'}$ and $b_0 = \langle b_{\mathbf{k}=0}\rangle$ obeying the supplementary equation $i\dot{b}_0 = E_0(B)b_0 + g_0\sum_{\mathbf{k}}\chi_{\mathbf{k}}(\sigma)\kappa_{\mathbf{k}}$. As with the single-channel theory, the five parameters which characterize the resonance, the background potential strength V_{bg} and range σ_{bg} (which define the entrance channel scattering length and its highest vibrational bound state), the interchannel coupling g_0 and its range σ, and the detuning $E_0(B)$ (which specify the position and width of the resonance), are determined from experiment and exact multichannel calculations [10].

Before turning to numerics, it is instructive to contrast our approach to that adopted in [5,7,8]. Given an initial condition, the Heisenberg equations (2) present a deterministic time evolution of the density distributions. Indeed, conservation of total density n, implicit in the dynamics (2), provides a check on the integrity of the numerical integration. By contrast, the integrability of the equations of motion as described by Refs. [5,7,8] relies on an additional constraint involving density and an auxiliary parameter playing the role of a "chemical potential." The constraint is needed in this case to fix the value of a momentum-dependent sign in the solution which should properly be determined by the initial conditions. A similar phenomenology describes the effect of a classical laser source on a semiconductor electron-hole system where the laser frequency "imprints" a chemical potential onto the system [12]: While equilibration processes are sufficiently small, the electrons and holes assume a nonequilibrium distribution around the externally imposed chemical potential resulting in a phenomenon of "spectral-hole burning" in which the density distribution is depleted at the laser frequency. In the atomic gas, where the degrees of freedom remain internal, it is difficult to see how such a choice is motivated or justified. Crucially, we will see that the unconstrained dynamics (2) lead to behavior very different from that obtained from the constrained [5,7,8].

With this background, let us now turn to the results of the numerical investigation of the dynamics (2). Although we

find that the qualitative behavior of BCS and BF dynamics is generic, we focus specifically on potentials tailored to the ^{40}K resonance at $B_0 = 202.1$ G with a density of $n = 1.5 \times 10^{13}$ cm^{-3} comparable to that used in experiment [2]. With these parameters, the equilibrium properties of the effective single-channel and BF models essentially coincide (for further details and values of parameters, we refer to Ref. [10]). Therefore, to keep our discussion concise, we focus on the single-channel theory, noting that the parallel application to the BF model with appropriate physical parameters generates *quantitatively* similar results.

At a field of ca. 1.0 G above the FR, the condensate has an essentially BCS-like character while the experiment using the fast sweep technique observed the condensate starting from 0.5 G above B_0. To explore the entire region of interest, we choose as initial conditions field values B_{I} which span the entire crossover region (marked by stars in Fig. 1). Starting from the ground state $T = 0$ distribution, we follow the dynamics of the condensate after an abrupt switch to some different value of magnetic field B_{F}.

Figure 2 shows the time evolution of $|\Delta_{\mathbf{k}=0}|$, normalized by Δ_{eq} (the value that it would acquire were the system to reach the $T = 0$ ground state at the final field B_{F}). Here we have chosen a field $B_{\mathrm{F}} - B_0 = -10$ G deep within the BEC phase where the large binding energy of molecules allows their momentum distribution to be inferred from time of flight measurements [2]. For comparison, insets of
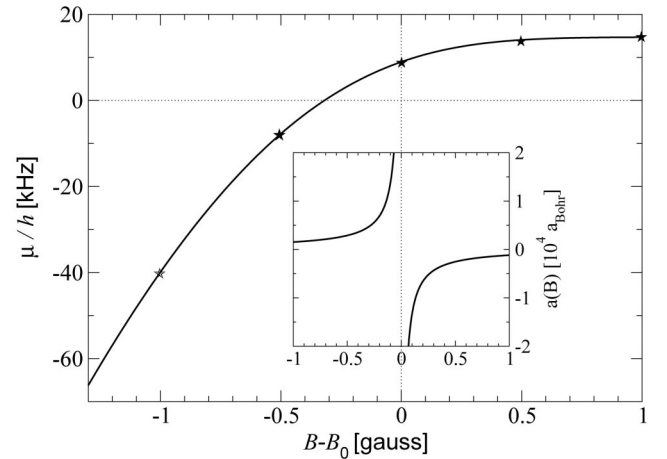

FIG. 1. Variation of the chemical potential μ with field B at $T = 0$ for a mixture of fermionic ^{40}K atoms prepared in the $(f = 9/2, m_f = -9/2)$ and $(f = 9/2, m_f = -7/2)$ Zeeman states at a density of $n = 1.5 \times 10^{13}$ cm^{-3} (i.e., $T_F = 0.35\ \mu$K). The FR takes place at $B_0 = 202.1$ G while the BEC-BCS crossover ($\mu = 0$) occurs when $B - B_0 \simeq -0.3$ G. Note that, since the density is nonzero, μ reaches zero below the two-body FR. The inset indicates the scattering length $a(B) = a_{\mathrm{bg}}(1 - \frac{\Delta B}{B-B_0})$ in the universal regime, where a_{bg} is the background potential scattering length and ΔB the width of the resonance. Note that, in the present theory, we use finite-range potentials with parameters which also describe the FR far beyond the universal region [10].

Fig. 2 show $B_F - B_0 = -1.0$ G. In contrast to the predictions of the constrained dynamics [5,7,8], these results show that (a) the coherent oscillations are substantially damped even at the mean-field level, (b) the amplitude of the oscillations is small, and (c) the order parameter $|\Delta_{\mathbf{k}=0}|$ asymptotes to a value much less than the expected final state equilibrium value Δ_{eq}. Referring to the insets of Fig. 2, one may note that, when the initial and final conditions are drawn closer, the period of the oscillations becomes longer and the effects of the damping more pronounced. Moreover, although the period of the oscillations decreases monotonically with Δ_{eq}, the dependence is nonlinear and, referring to the bottom inset of Fig. 3, one may note that Δ_{eq} does not provide a ceiling for the magnitude of the oscillation.

To interpret the generic behavior, it is instructive to access the time dependence of the pair wave function $\kappa_{\mathbf{k}}$
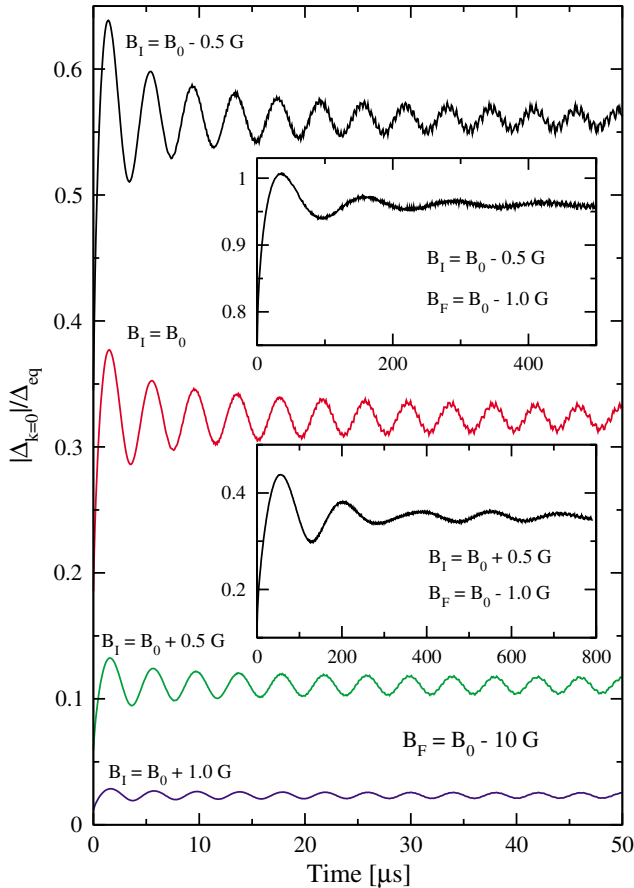
and the distribution $\Phi_{\mathbf{k}}$. Figure 3 shows that, when the abrupt switch takes place from $B_I - B_0 = 0.5$ G to $B_F - B_0 = -10$ G, although there is a slight tendency to shift towards the final state equilibrium distribution, the pair wave function and the density distribution remain essentially frozen close to the initial BCS-like distribution, exhibiting only small oscillations in time. In the absence of energy relaxational processes, the system is unable to significantly redistribute weight. By contrast, when the switch takes place from $B_I - B_0 = 0.5$ G to

FIG. 2 (color online). Time dependence of the order parameter $|\Delta_{\mathbf{k}=0}|/\Delta_{eq}$ following an abrupt switch from a field of $(B_I - B_0)/G = -0.5$ (top), 0.0, 0.5, 1.0 (bottom) to $(B_F - B_0)/G = -10$, and from $(B_I - B_0)/G = -0.5$ (top inset) and $(B_I - B_0)/G = 0.5$ (bottom inset) to $(B_F - B_0)/G = -1.0$. In addition to the constant phase velocity of $\Delta_{\mathbf{k}=0}$ (found numerically to be set by the final state equilibrium μ), there is an additional time-dependent phase modulation whose characteristics mirror closely that of the amplitude oscillations.
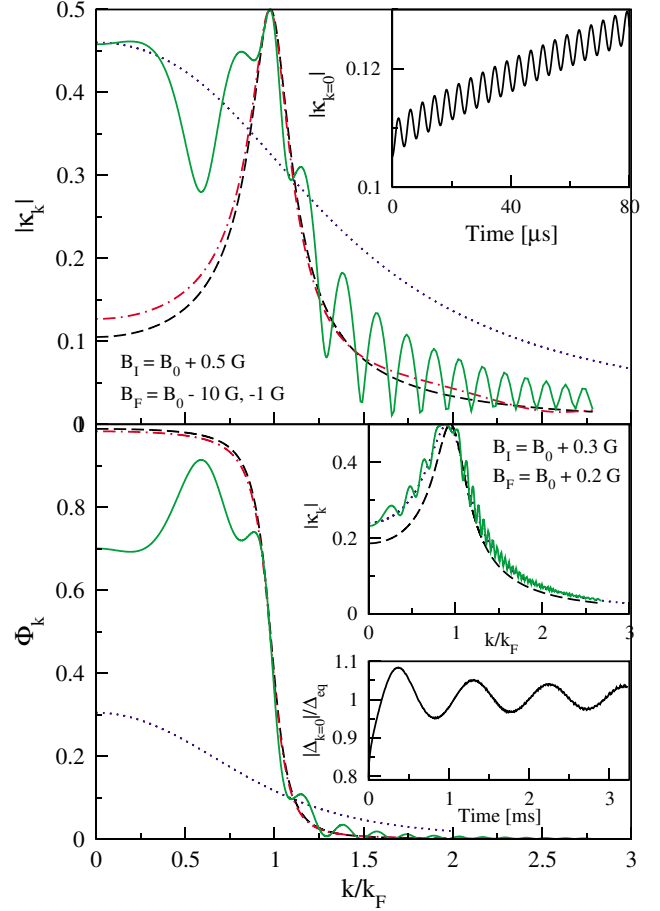

FIG. 3 (color online). The pair wave function $|\kappa_{\mathbf{k}}|$ (upper panel) and the density distribution $\Phi_{\mathbf{k}}$ (lower panel) shown as a function of $k = |\mathbf{k}|$ with $B_I - B_0 = 0.5$ G (dashed lines) and $B_F - B_0 = -10$ G after $50\ \mu$s (dash-dotted line) and $B_F - B_0 = -1.0$ G after $800\ \mu$s (solid line) following the abrupt switch as in Fig. 2. The dotted lines signify the ground state equilibrium distributions at $B_F - B_0 = -1.0$ G included for comparison. The upper inset shows oscillations of $|\kappa_{\mathbf{k}=0}|$ for $B_F - B_0 = -10$ G. The lower two insets refer to a weak perturbation on the BCS side from $B_I - B_0 = 0.3$ G (dashed line) to $B_F - B_0 = 0.2$ G. The dotted line shows the equilibrium distribution while the solid line provides a snapshot of the distribution at 3 ms after the switch. Note that the harmonic modulations visible in the distribution functions translate to a single energy scale of the same order of magnitude as the period of oscillations seen in $|\Delta_{\mathbf{k}=0}|$.
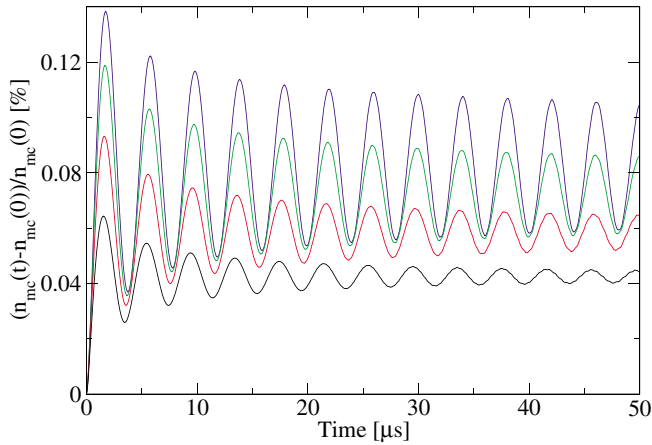
FIG. 4 (color online). Time dependence of the condensed molecule density $[n_{mc}(t) - n_{mc}(0)]/n_{mc}(0)$. Here we have used the same field values as that used in Fig. 2 (main) with $(B_I - B_0)/G = -0.5$ (top), 0.0, 0.5, and 1.0 (bottom) and $(B_F - B_0)/G = -10$. When normalized to one-half of the total atomic density, $n_{mc}(0) = 0.3, 0.1, 0.012,$ and 0.0005, respectively.

$B_F - B_0 = -1.0$ G, the proximity of the two phases allows the system to converge to a (nonstationary) modulated distribution whose (stationary) envelope reflects more closely the final state equilibrium distribution. The lower insets in Fig. 3 show that a weakly perturbed condensate on the BCS side approaches equilibrium with the pair distribution showing small modulations around the equilibrium one in accord with the linear stability analysis of the weakly perturbed BCS system (2) (Refs. [13,14]). In particular, one may note that here (and, indeed, for other initial and final conditions) the hole-burning predicted by the constrained dynamics [8] does not appear.

To assess the potential of observing coherent atom-molecule oscillations, we now look at the time evolution of the number of condensed molecules, $n_{mc}(t) = |\int d^3k \kappa_k(t) \phi_B(k, B_F)|^2$. Here $\phi_B(k, B_F)$ is the wave function of the highest bound eigenstate of the two-body problem [10]. Referring to Fig. 4, we see that the amplitude of oscillations is negligible. Although one may adjust the final field B_F to lie closer to the FR, the amplitude of the oscillations increases only slightly while the damping rate is enhanced. Moreover, the inclusion of processes beyond mean field would simply increase the damping rate and not enhance the oscillations. We therefore conclude that the observation of atom-molecule oscillations, after an abrupt change in the interaction strength, is infeasible for the entrance channel dominated resonances currently studied in ^{40}K and ^{6}Li.

To conclude, we have presented a numerical analysis of the dynamical mean-field equations for the single-channel theory of the FR following an abrupt field change. In the range of physical parameters appropriate to the ^{40}K system, consideration of the two-channel BF theory does not change the results. When applied to a theoretical regime where the population of the closed channel states below

resonance is high, the numerical findings do not change *qualitatively.* Relying on the deterministic time evolution of the initial state according to the Heisenberg equations, our results differ substantially from the findings of the constrained dynamics [5,7,8]. Over a wide range of initial conditions, we observe substantially damped oscillations with an amplitude strongly dependent on initial conditions and a frequency set by the interaction strength after the switch. To assess the capacity for BCS-BEC-like atom-molecule oscillations following an abrupt change in the interaction, we have chosen initial and final conditions to span the crossover from the BCS to the BEC limits. We have found that the amplitude of atom-molecule oscillations is negligible and the distribution is essentially frozen to the initial one, a behavior reminiscent of an orthogonality catastrophe. We conclude that, in the entrance channel dominated resonances observed in ^{40}K and ^{6}Li, BCS-BEC atom-molecule oscillations cannot be observed. The rigidity of the condensate wave function distribution at short-time scales, where the time evolution is mean field in character, supports the method of the fast sweep as a reliable technique to probe the fermionic pair condensate.

[1] M. Greiner *et al.*, Nature (London) **426**, 537 (2003); S. Jochim *et al.*, Science **302**, 2101 (2003); M. W. Zwierlein *et al.*, Phys. Rev. Lett. **91**, 250401 (2003).
[2] C. A. Regal *et al.*, Phys. Rev. Lett. **92**, 040403 (2004).
[3] M. W. Zwierlein *et al.*, Phys. Rev. Lett. **92**, 120403 (2004).
[4] E. A. Donley *et al.*, Nature (London) **417**, 529 (2002).
[5] R. A. Barankov *et al.*, Phys. Rev. Lett. **93**, 160401 (2004).
[6] E. A. Yuzbashyan *et al.*, cond-mat/0407501.
[7] R. A. Barankov *et al.*, Phys. Rev. Lett. **93**, 130403 (2004).
[8] A. V. Andreev *et al.*, Phys. Rev. Lett. **93**, 130402 (2004).
[9] K. Góral *et al.*, J. Phys. B **37**, 3457 (2004).
[10] M. H. Szymańska *et al.*, cond-mat/0501728 [Phys. Rev. A (to be published)].
[11] M. Holland *et al.*, Phys. Rev. Lett. **87**, 120406 (2001); E. Timmermans *et al.*, Phys. Lett. A **285**, 228 (2001); Y. Ohashi *et al.*, Phys. Rev. Lett. **89**, 130402 (2002).
[12] S. Schmitt-Rink *et al.* Phys. Rev. B **37**, 941 (1988).
[13] A. F. Volkov and Sh. M. Kogan, Sov. Phys. JETP **38**, 1018 (1974).
[14] In this context, it would be interesting to explore the potential connection between the weak coherent oscillations and equilibrium quantum fluctuations [15] found above and below T_c in the BF system.
[15] Y. Ohashi and A. Griffin, Phys. Rev. A **67**, 063612 (2003); T. Domanski and J. Ranninger, Phys. Rev. B **70**, 184503 (2004).